ELSEVIER

Polymer 42 (2001) 3213–3221

polymer

www.elsevier.nl/locate/polymer

Hydrogen bonding and mechanical properties in segmented montmorillonite/polyurethane nanocomposites of different hard segment ratios

Y.I. Tien, K.H. Wei*

Department of Materials Science and Engineering, National Chiao Tung University, Hsinchu 30049, Taiwan, Republic of China

Received 16 May 2000; received in revised form 17 July 2000; accepted 10 August 2000

Abstract

Hydrogen bonding in the hard segments of the synthesized montmorillonite/polyurethane nanocomposites of various hard segment ratios was found to decrease with the increasing amount of montmorillonite regardless of the hard segment ratios, but reached plateau values at 5 wt% montmorillonite concentration. The maximal reductions of the hydrogen bonding in the polyurethane nanocomposites ranged from 20 to 37%, depending on the hard segment ratios as compared to that in the pure polyurethane. The maximal strength and the elongation at break of the polyurethane nanocomposites increased dramatically as compared to that of pristine polyurethane, and the maximal values occurred at 1 wt% montmorillonite concentration.

Keywords: Polyurethane; Nanocomposites; Hydrogen bonding

1. Introduction

Conventional composites have been widely used in such diverse areas as transportation, construction, electronics and consumer products. The constituents of composites can be two or more kinds of materials possessing complementary physical and chemical properties, and they are expected to produce a synergistic property, which is difficult to attain separately from that of the individual components. Composites having more than one solid phase with a dimension in the 1–20 nm range [1–4] are defined as nanocomposites. Nanocomposites are a new class of materials having better physical properties such as thermal, mechanical and barrier properties than that of conventional composites because of the much stronger interfacial forces between the well-dispersed nanometer-sized domains.

Natural montmorillonite consisted of layers made up of two silicate tetrahedron fused to an edge-shared octahedral sheet of either aluminum or magnesium hydroxide. The physical dimensions of these disc-like shaped silicate layers were approximately 100 nm in diameter and 1-nm thick. Stacking of the silicate layers leads to a regular van der Waals gap between the layers, which was termed as the interlayer gallery. Isomorphic substitution within the layers generates negative charges that are normally counterbalanced by cations (Na^+, Ca^{2+}, or K^+) residing in the gallery space [5]. Since montmorillonite is hydrophilic and lacks affinity with hydrophobic organic polymers, ion exchange reactions of montmorillonite with various organic cations such as alkylammonium cations rendered the originally hydrophilic silicate surfaces hydrophobic. The organic cations lowered the surface energy of silicate layers and enhanced the miscibility between the silicate layers and the polymer matrix.

After the development of montmorillonite/Nylon 6 [6–10] nanocomposite by Toyota in 1990 in Japan, a number of condensation polymer nanocomposites has been synthesized [11–20]. Thermoplastic polyurethane copolymer consisting of alternating flexible and rigid segments displayed a two-phase morphology due to the segmental incompatibility. The factors influencing the phase separation of polyurethane were the segmental length, the crystallizability of the segment, the intra- and inter-segments interaction, the overall composition and the molecular weight. The segmented natures of polyurethane [21–23] and polyurethaneurea [24,25] usually were studied with differential scanning calorimetry (DSC), Fourier transformed infrared spectroscopy (FTIR) and wide angle X-ray diffraction (WAXD).

Recently, we developed montmorillonite/polyurethane nanocomposites by treating the synthesized low molecular

* Corresponding author. Tel.: +886-35-731871; fax: +886-35-724727.
E-mail address: khwei@cc.nctu.edu.tw (K.H. Wei).

0032-3861/01/$ - see front matter
PII: S0032-3861(00)00729-1

Table 1
Composition and number molecular weight of polyurethane and BZD-Mont/polyurethane nanocomposites

	Molar ratio (MDI/1,4-BD/PTMEG)	BZD-Mont ratio (wt%)	Molecular weight (M_n)
PU39	2/1/1	0	13,900
1/99 BZD-Mont/PU39	2/1/1	1	14,500
3/97 BZD-Mont/PU39	2/1/1	3	15,400
5/95 BZD-Mont/PU39	2/1/1	5	15,100
PU50	3/2/1	0	15,600
1/99 BZD-Mont/PU50	3/2/1	1	14,800
3/97 BZD-Mont/PU50	3/2/1	3	13,100
5/95 BZD-Mont/PU50	3/2/1	5	15,200
PU63	5/4/1	0	13,600
1/99 BZD-Mont/PU63	5/4/1	1	13,700
3/97 BZD-Mont/PU63	5/4/1	3	15,100
5/95 BZD-Mont/PU63	5/4/1	5	15,900

weight montmorillonite/polycaprolactone nanocomposites as the soft segments in a two-step synthesis [17]. Moreover, the montmorillonite/polyurethane nanocomposites can also be synthesized directly by dispersing the organics-modified silicate layers in polyurethane [18]. These montmorillonite/polyurethane nanocomposites displayed enhanced mechanical, thermo-degradation and water absorption properties than that of the pure polyurethane. However, the presence of layered silicates must have affected the degree of phase separation (DPS) and the hydrogen bonding of montmorillonite/polyurethane nanocomposites. The objective of this study is to examine the effect of montmorillonite on the hydrogen bonding extent and the mechanical properties of montmorillonite/polyurethane nanocomposites of different hard segment ratios synthesized by a one-step method.

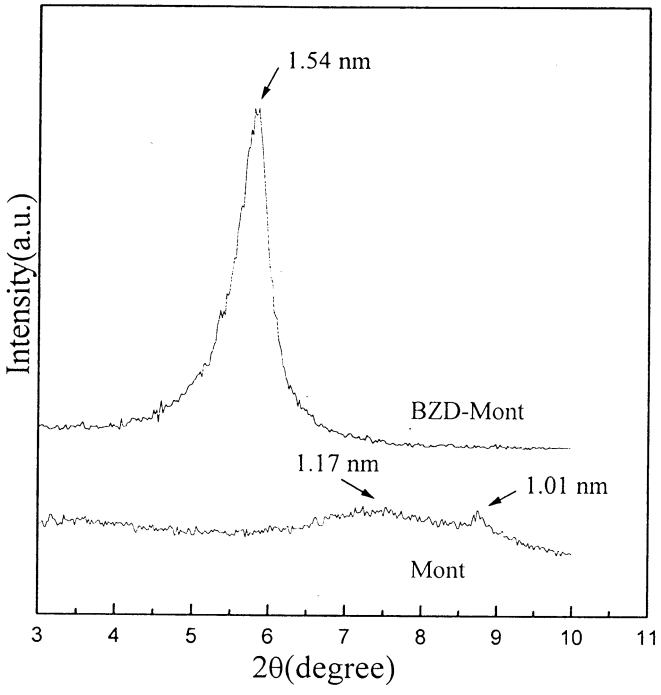

Fig. 1. The wide angle X-ray diffraction patterns of benzidine-modified-montmorillonite (BZD-Mont) and montmorillonite (Mont).

2. Experimental section

2.1. Materials

Wyoming Na^+-montmorillonite, Source clay Swy-2, was obtained from the Clay Minerals Depository at the University of Missouri, Columbia, MO, USA. Swy-2 Na^+-montmorillonite having a cationic exchange capacity 76.4 meq/100 g was screened with a sieve of 325-mesh to remove impurities. 10 g of the screened montmorillonite was gradually added to a previously prepared solution of 0.89 g benzidine dissolved in 1000 ml of 0.01 N HCl at 60°C, and the resultant suspension was vigorously stirred for 3 h. The treated montmorillonite was repeatedly washed by de-ionized water. The filtrate was titrated with 0.1 N $AgNO_3$ until the formation of AgCl precipitate occured no more, to ensure the complete removal of chloride ions. The filtered cake was then placed in a vacuum oven at 80°C for 12 h drying. The dried cake was ground and screened with a 325-mesh sieve to obtain the benzidine-modified-montmorillonite which was termed BZD-Mont.

Polytetramethylene glycol (PTMEG, $M_n = 1000$, Aldrich) was dehydrated under a vacuum oven at 60°C for two days. 4,4′-diphenylmethane diisocyanate (MDI, Aldrich) was melted and pressure filtered under N_2 at 60°C followed by recrystallization from hexane in an ice bath. Dimethylforamide (DMF, 99%, Fisher) and 1,4-butanediol (1,4-BD, Lancaster) were dried over calcium hydride for two days and then were vacuum-distilled. Pure polyurethane of different hard segment ratios was produced by a random one-step method in which MDI, 1,4-BD and PTMEG were directly mixed in DMF [22], and then the whole solution was heated to 90°C for 3 h. Subsequently, the polyurethane solution was cooled back to room temperature, and 10 ml DMF was added to the solution followed by more stirring for 3 h to complete the reaction. The final concentration of polyurethane in DMF was 30 wt% by weight. For preparing the montmorillonite/polyurethane nanocomposites, different amounts of BZD-Mont were mixed with 10 ml of DMF, and the BZD-Mont/DMF was added to the previously prepared polyurethane solution with stirring for 3 h at room temperature. The pristine polyurethane and the BZD-Mont/polyurethane nanocomposite films were obtained by casting the solutions in a mold at 70°C for 24 h. The compositions of the montmorillonite/polyurethane nanocomposites are given in Table 1.

2.2. Characterization

WAXD experiments were performed by using Mac Science M18 X-ray diffractometer. The X-ray beam was

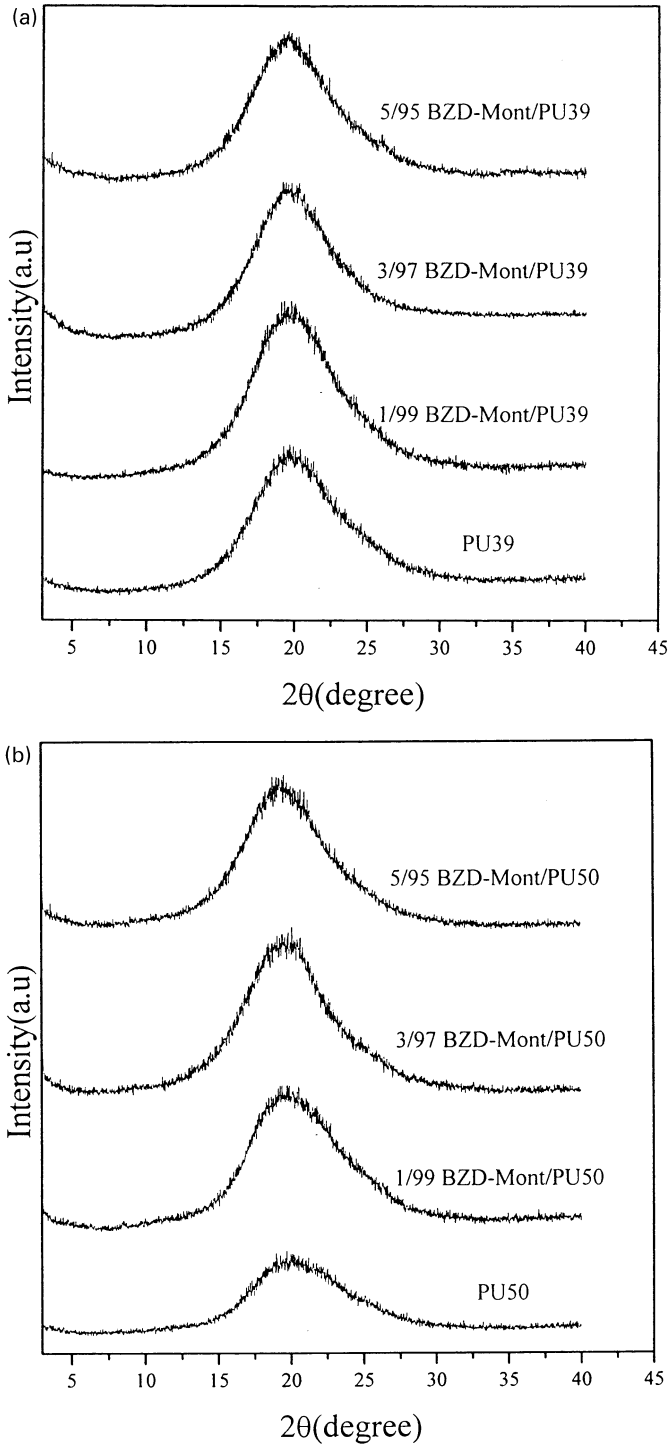

Fig. 2. The wide angle X-ray diffraction patterns of pristine polyurethane and of BZD-Mont/polyurethane for: (a) PU39; (b) PU50; and (c) PU63 cases.

derived from nickel-filtered Cu Kα ($\lambda = 0.154$ nm) radiation in a sealed tube operated at 50 kV, 250 mA, and the diffraction curves were obtained from 3 to 40° at a scan rate of 1°/min. The molecular weights of the recovered [19] and the pristine polyurethane were determined by Waters 510 Gel Permeation Chromatography (GPC) with DMF as the solvent. The calibration curves for GPC were obtained by using polystyrene and polyethylene glycol standards. FTIR experiments were performed with a Nicolet Ominc 3 spectrometer at a resolution of 4 cm^{-1}. Polyurethane and BZD-Mont/polyurethane nanocomposites solutions were coated on KBr discs, and then the discs were put in a vacuum oven at 70°C for 24 h to remove DMF for FTIR studies. Tensile strength tests were carried out on the samples with

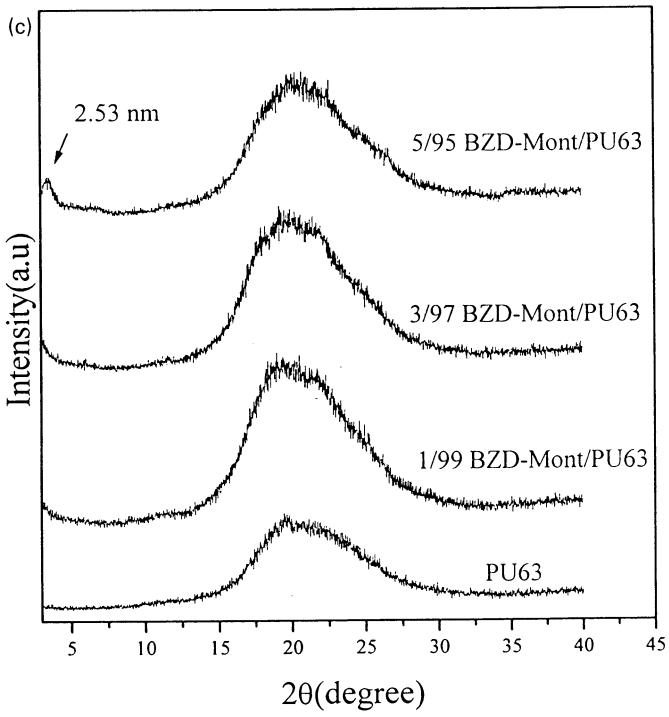

Fig. 2. (*continued*)

Instron 4468 machine according to the specifications of ASTM D882. The shapes of samples were $100 \times 10 \times 1\ mm^3$ in size, and the crosshead speed was set at 500 mm/min. For each data point, five samples were tested, and the average value was taken. The samples for transmission electron microscopy (TEM) study were first prepared by putting BZD-Mont/polyurethane nanocomposites into epoxy capsules, and then it was cured at 70°C for 24 h in a vacuum oven to avoid inducing stress on the samples. The cured epoxies containing BZD-Mont/polyurethane nanocomposites were microtomed with Leica Ultracut Uct into about 90 nm thick slices at −80°C. A carbon layer of 3 nm thickness was deposited on these slices that were being kept on 200-mesh copper nets for TEM observation. The type of TEM used is JEOL-200FX.

3. Results and discussion

The WAXD curves of the montmorillonite and the BZD-Mont were presented in Fig. 1. In Fig. 1, the *d*-spacings of the pristine montmorillonite and the BZD-Mont were 1 and 1.54 nm, respectively, indicating that the silicate layer galleries in the montmorillonite were intercalated by benzidine molecules. The *d*-spacing of BZD-Mont is smaller than the benzidine molecular length (1.8 nm), which is caused by benzidine being oriented slightly diagonally to the in-plane direction of silicate layers [7,26]. The WAXD patterns of PU39, PU50 and PU63 nanocomposites containing different amounts of BZD-Mont are shown in Fig. 2(a)–(c), respectively. In Fig. 2(a)–(c), there were no diffraction peaks appearing between $2\theta = 3$ to 6° except in the case of 5/95 BZD-Mont/PU63, implying that silicate layers were intercalated by the polyurethane molecules in these cases. The relatively small diffraction peak displayed at $2\theta = 3.5°$ in the WAXD pattern of 5/95 BZD-Mont/PU63 corresponded to a *d*-spacing of 2.53 nm. This anomaly can be explained by the fact that as the hard segment ratio in the polyurethane molecules increased, the molecules became more rigid and had difficulty in diffusing into the silicate layer galleries for intercalation. A very diffused diffraction peak near $2\theta = 19°$ appeared for all polyurethane nanocomposites of different hard segment ratios. This weak peak is attributed to a short-range-order arrangement of chain segments [22,25,27–29] of polyurethane molecules. Further evidence of the formation of the BZD-Mont/polyurethane nanocomposites can be found in the transmission electron micrographs as shown in Fig. 3. In Fig. 3(a)–(c), the average spaces between the silicate layers in 1/99 BZD-Mont/PU39, 1/99 BZD-Mont/PU50 and 5/95 BZD-Mont/PU50 are about 10, 5 and 3 nm, respectively. These spaces between the silicate layers in polyurethane are much larger, 1 nm, than that in the pristine montmorillonite and decrease with the increasing amount of either the hard segment or BZD-Mont in polyurethane.

The molecular weights of recovered [19] polyurethane from the nanocomposites were given in Table 1. In Table 1, the variations in the molecular weight of polyurethane at different compositions were less than 10%, indicating that the polyurethane molecular chain lengths were not affected by the presence of the silicate layers. The degree of hydrogen bonding in these polyurethane nanocomposites can be

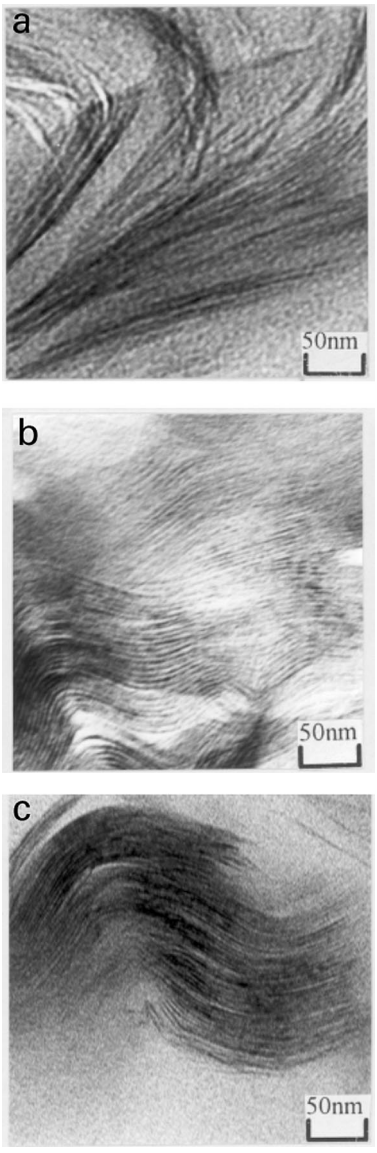

Fig. 3. Transmission electron micrographs of the cross-section views of: (a) 1/99 BZD-Mont/PU39; (b) 1/99 BZD-Mont/PU50; and (c) 5/95 BZD-Mont/PU63.

obtained from their IR spectra. The IR spectra of PU39, PU50 and PU63 nanocomposites containing different amount of BZD-Mont are shown in Fig. 4(a)–(c), respectively. In Fig. 4(a)–(c), the positions of bands for distinctive functional groups in the IR spectra of the pristine polyurethane and the BZD-Mont/polyurethane nanocomposites are identical, confirming that the chemical structures of polyurethane were not altered by the presence of silicate layers. Therefore, the effect of the intercalated silicate layers on the degree of phase separation in polyurethane can be determined solely from the extent of hydrogen bonding in the hard segments. The detailed description of IR bands in polyurethane can be found elsewhere [21], and only the relevant ones are discussed here. The infrared bands at 3480 and 3320 cm^{-1} are due to the free N–H stretching and the hydrogen-bonded N–H stretching in the polyurethane, respectively. The 1733 cm^{-1} band is caused by the free-of-hydrogen-bonding carbonyl, and the band at 1703 cm^{-1} is associated with the hydrogen-bonded carbonyls. The characteristic absorbances have been normalized by taking the sample thickness into account using the C–H absorbance at 2935 cm^{-1} as the standard. For each curve in Fig. 4(a)–(c), there was a band located at 3320 cm^{-1}, and no band appeared at 3480 cm^{-1}, indicating that the N–H groups in the polyurethane nanocomposites were nearly completely hydrogen-bonded. The possible functional groups acting as the acceptors in the hydrogen bonding with N–H are the urethane carbonyl (–C═O), the ether (–C–O–C–) and the oxygen of the hydroxyl groups (–OH) on silicate layers. The degree of the carbonyl groups participating in hydrogen bonding can be described by the carbonyl hydrogen bonding index, R, as given in Eq. (1).

$$R = \frac{C_{\text{bonded}}\epsilon_{\text{bonded}}}{C_{\text{free}}\epsilon_{\text{free}}} = \frac{A_{1703}}{A_{1733}} \tag{1}$$

where A is the intensity of the characteristic absorbance, C is the concentration and ϵ_{bonded} and ϵ_{free} are the extinction coefficients of the bonded and the free carbonyl groups, respectively. The value of $\epsilon_{\text{bonded}}/\epsilon_{\text{free}}$ was between 1.0 and 1.2 [21,30]. In this study, the value of $\epsilon_{\text{bonded}}/\epsilon_{\text{free}}$ is taken as 1.0, and the carbonyl hydrogen bonding index is directly equal to the ratio of the normalized absorbance intensity in 1703 cm^{-1} to that in 1733 cm^{-1}. The degree of hard segment linking hard segment (degree of phase separation, DPS) and the degree of hard segment linking soft segment or silicate layers (degree of phase mixing, DPM) can be obtained readily by using Eqs. (2) and (3), respectively [21,30,31].

$$DPS = \frac{C_{\text{bonded}}}{C_{\text{bonded}} + C_{\text{free}}} = \frac{R}{R+1} \tag{2}$$

$$DPM = 1 - DPS \tag{3}$$

The obtained values of R, DPS and DPM for BZD-Mont/polyurethane nanocomposites were given in Table 2. In Table 2, the degree of hydrogen bonding of carbonyl groups and the resultant DPS increased with the hard segment ratios in the pristine polyurethane. This result is consistent with the previous reports in the literatures [22,24]. The hydrogen bonding indices of 1/99 BZD-Mont/PU39, 1/99 BZD-Mont/PU50, 1/99 BZD-Mont/PU63 are smaller than that of pristine polyurethane. Therefore, the DPS in BZD-Mont/polyurethane nanocomposites was reduced in the presence of a small amount of silicate layers. Moreover, the hydrogen bonding index of carbonyl groups in BZD-Mont/polyurethane regardless of their hard segment ratios, decreased with the increasing amount of BZD-Mont but seemed to reach plateau values at 5 wt% BZD-Mont concentration. The maximal reductions in the carbonyl hydrogen bonding index for PU39, PU50 and PU63 nanocomposites were 20, 34 and 37%, respectively. This phenomenon can be manifested by a close

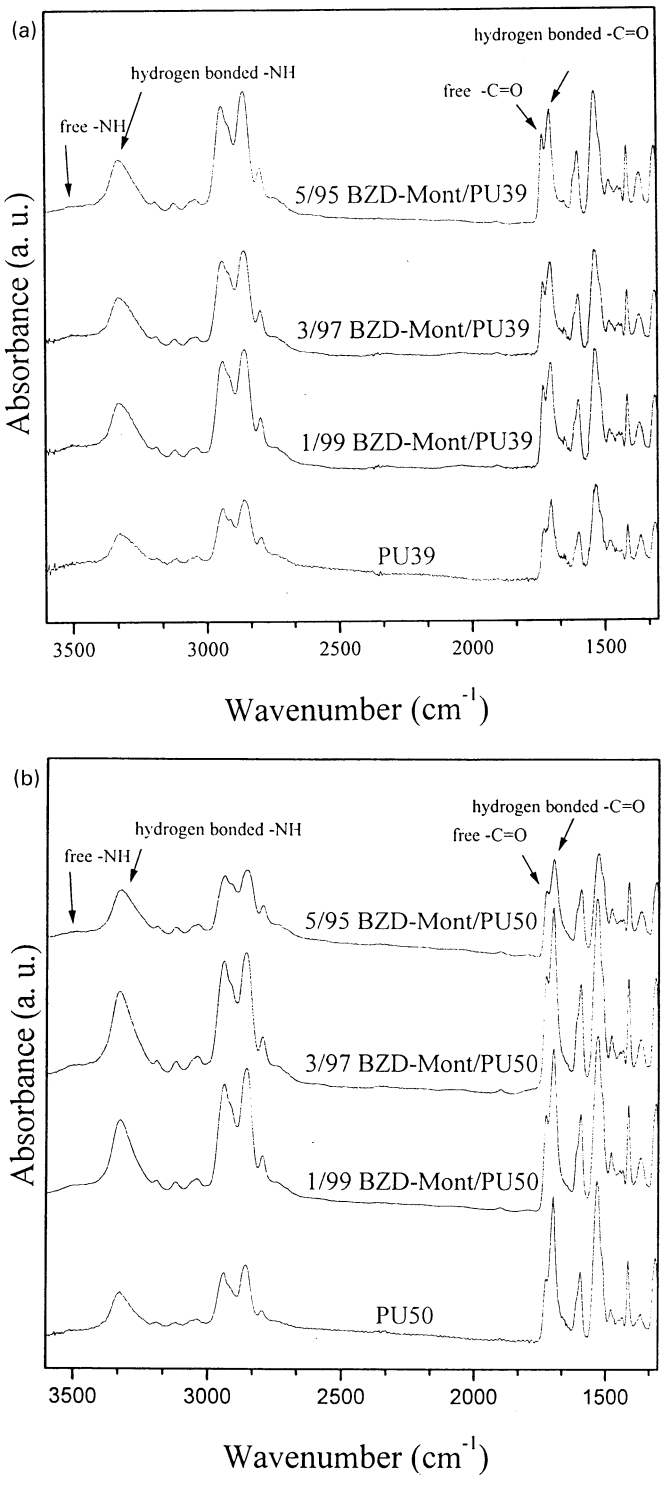

Fig. 4. The Fourier transformed infrared spectra of BZD-Mont/polyurethane for: (a) PU39; (b) PU50; and (c) PU63 cases.

examination of the morphology of these nanocomposites. The nanometer-scale silicate layers dispersed in polyurethane created large interfacial areas where the hydroxyl groups on the silicate layers can form hydrogen bonding with either the hard or the soft segments in polyurethane. Since the rigid silicate layers retarded the mobility of the hard segments more than that of the soft segments, the forming of the hydrogen bonding between the hard segments of polyurethane in these interfacial areas was therefore obstructed. The intercalation of the silicate layers by polyurethane molecules decreased when the amount of BZD-Mont increased as evidenced in the TEM

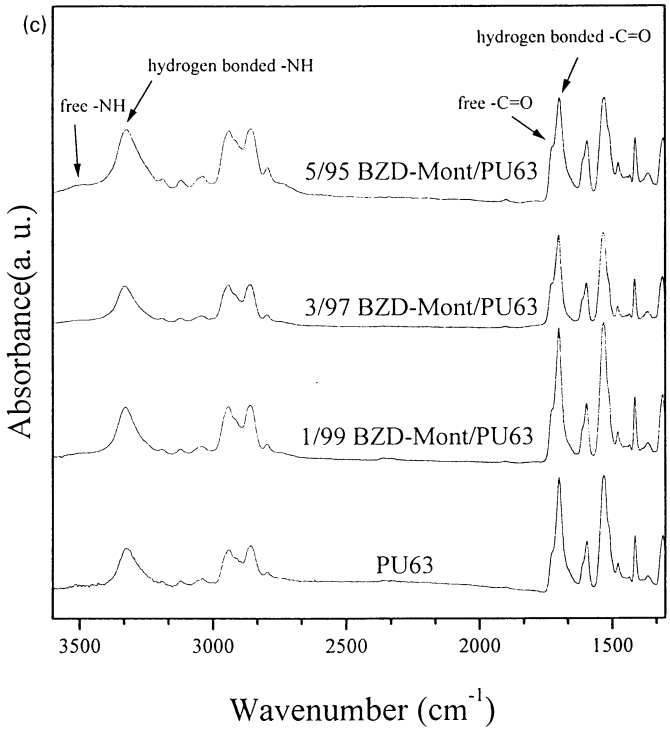

Fig. 4. (*continued*)

micrographs in Fig. 3(b) and (c). Hence, the extent of the disruption by silicate layers on the formation of hydrogen bonding between the hard segments became diminished as the amount of silicate layers increased.

In Table 3, the maximal strength of PU39, PU50 and PU63 nanocomposites containing 1 wt% BZD-Mont were 29, 70 and 46% larger than that of pristine PU39, PU50 and PU63, respectively. The presence of the silicate layers tended to reinforce the polyurethane, but also reduced the hydrogen bonding between the hard segments i.e. the amount of hard segments. Consequently, the optimal maximal strength occurred at 1 wt% BZD-Mont in polyurethane. The schematics of possible dispersions of the silicate layers in polyurethane are presented in Fig. 5(a)–(c). In Fig. 5(a), the morphology of the pristine segmented polyurethane was illustrated. The speculated morphologies of the well- and the poorly-dispersed silicate layers in the segmented polyurethane in Fig. 5(b) and (c), respectively, corresponded to 1/99 and 5/95 BZD-Mont/polyurethane. The elongation at break of the nanocomposites with 1 wt% BZD-Mont in PU39, PU50 and PU63 were 27, 69 and 35% higher than that of pure PU39, PU50 and PU63, respectively, as shown in Table 3. The presence of silicate layers tends to enhance

Table 2
The carbonyl hydrogen bonding index, the degree of phase separation (DPS) and the degree of phase mixing (DPM) in BZD-Mont/polyurethane nanocomposites

	A_{1703}/A_{1733}[a]	DPM	DPS
PU39	1.58	39	61
1/99 BZD-Mont/PU39	1.29	44	56
3/97 BZD-Mont/PU39	1.28	44	56
5/95 BZD-Mont/PU39	1.27	44	56
PU50	2.26	30	70
1/99 BZD-Mont/PU50	1.67	37	63
3/97 BZD-Mont/PU50	1.59	39	61
5/95 BZD-Mont/PU50	1.49	40	60
PU63	2.93	25	75
1/99 BZD-Mont/PU63	2.48	29	71
3/97 BZD-Mont/PU63	2.10	32	68
5/95 BZD-Mont/PU63	1.86	35	65

[a] A_{1733}, absorption intensity of free carbonyl; A_{1703}, absorption intensity of hydrogen-bonded carbonyl; A_{1703}/A_{1733}, carbonyl hydrogen bonding index.

Table 3
The tensile properties of BZD-Mont/polyurethane nanocomposites containing different hard segment ratios and BZD-Mont contents

	Maximal strength (kgf/cm^2)	Modulus (kgf/cm^2)	Elongation at break (%)
PU39	62.9	218	480
1/99 BZD-Mont/PU39	81.0	265	610
3/97 BZD-Mont/PU39	72.8	221	599
5/95 BZD-Mont/PU39	66.2	218	593
PU50	107.5	1324	205
1/99 BZD-Mont/PU50	182.6	1621	346
3/97 BZD-Mont/PU50	169.4	1607	294
5/95 BZD-Mont/PU50	166.0	1584	216
PU63	138.1	1679	140
1/99 BZD-Mont/PU63	201.4	1931	189
3/97 BZD-Mont/PU63	180.3	1906	185
5/95 BZD-Mont/PU63	162.3	1762	151

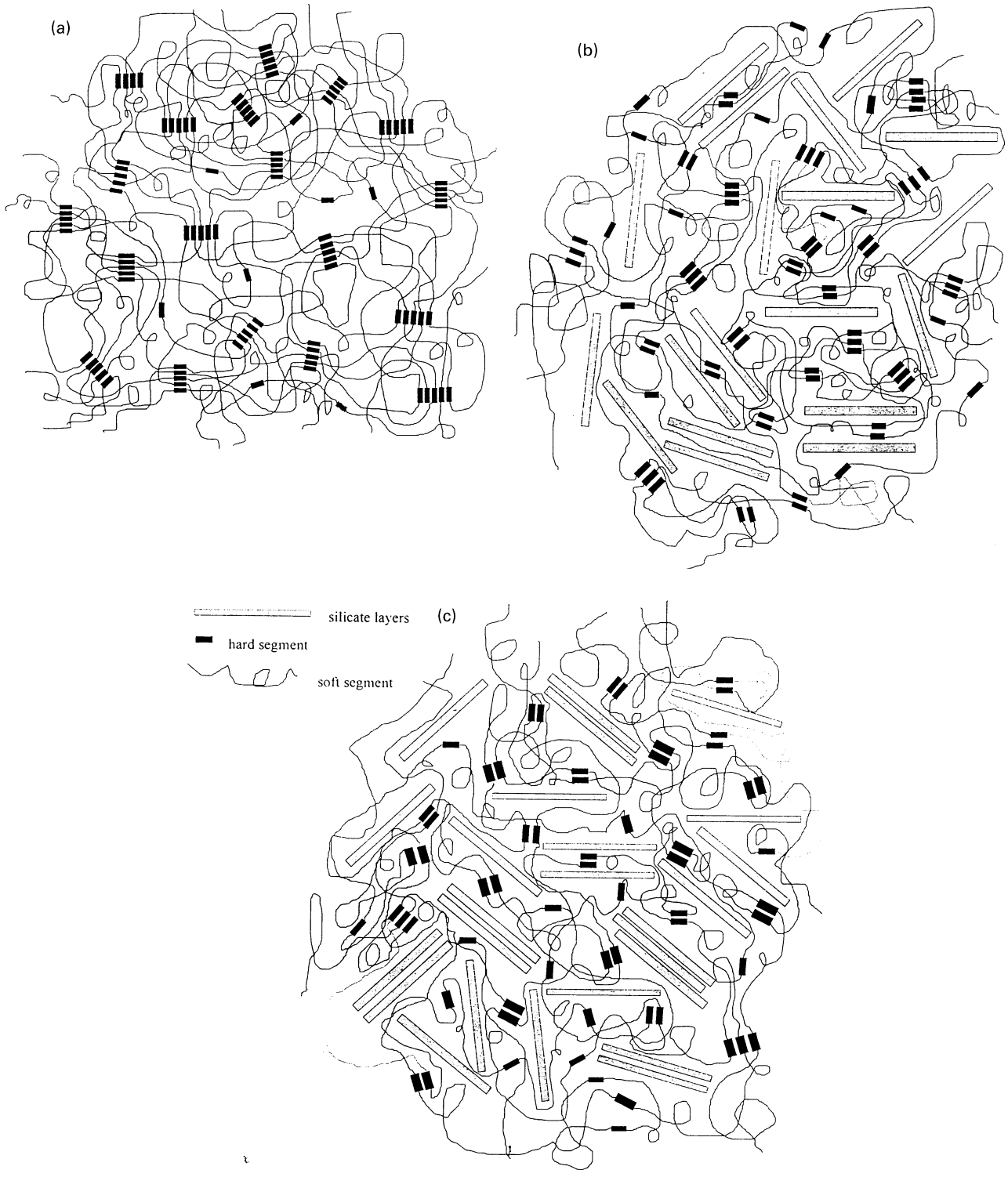

Fig. 5. The schematic drawing of the morphology of: (a) pristine polyurethane; (b) well-dispersed BZD-Mont in polyurethane nanocomposite; and (c) poorly-dispersed BZD-Mont in polyurethane nanocomposite.

the maximal strength of pure polyurethane as occurred in some cases of conventional composite materials. For the same BZD-Mont/polyurethane nanocomposites, the elongation behavior was determined by the interfacial interaction between polyurethane and BZD-modified-silicates where the gallery onium ions [15] contributed to the dangling chain formation in the matrix and caused a plasticizing effect in polyurethane. Therefore, the maximal strength and elongation at break of BZD-Mont/polyurethane nanocomposites enhanced simultaneously. Due

to the poorer dispersion of montmorillonite/polyurethane nanocomposites containing more BZD-Mont, the elongation enhancement decreased with the BZD-Mont content. The Young's modulus of BZD-Mont/polyurethane nanocomposites had the modest gain, about 20%, as compared to that of pure polyurethane at various hard segment ratios as given in Table 3, due to the stiffness of the silicate layers.

4. Conclusions

The degree of hydrogen bonding in the hard segments in polyurethane was reduced due to the presence of the silicate layers, and the resultant morphology of the segmented polyurethane was altered. The extent of the reduction between the hydrogen bonding in the hard segment depends on the amount of the silicate layers and their dispersion. The combination of the reinforcing effect of the silicate layers and its effect on the morphology of polyurethane resulted in an optimal enhancement of the maximal strength and the elongation at break, regardless of their hard segment ratios.

Acknowledgements

The authors appreciated the financial support provided by the National Science Council through Project NSC89-2216-E-009-008.

References

[1] Komarneni SJ. Mater Chem 1992;2:1219.
[2] Gleiter H. Adv Mater 1992;4:474.
[3] Novak BM. Adv Mater 1993;5:422.
[4] Ziolo RF, Giannelis EP, Weinstein BA, O'Horo MP, Granguly BN, Mehrota V, Russell MW, Huffman DR. Science 1992;257:219.
[5] Giannelis EP. Adv Mater 1996;8:29.
[6] Usuki A et al. US Pat. 4889885, 1989.
[7] Usuki A, Kawasumi M, Kojima Y, Okada A, Kurauchi T, Kamigaito O. J Mater Res 1993;8:1174.
[8] Usuki A, Kawasumi M, Kojima Y, Okada A, Fukushima Y, Kurauchi T, Kamigaito O. J Mater Res 1993;8:1179.
[9] Kojima Y, Usuki A, Kawasumi M, Okada A, Kurauchi T, Kamigaito O. J Polym Sci A: Polym Chem 1993;31:983.
[10] Kojima Y, Usuki A, Kawasumi M, Okada A, Kurauchi T, Kamigaito O. J Polym Sci A: Polym Chem 1993;31:1755.
[11] Yano K, Usuki A, Okada A, Kurauchi T, Kamigaito O. J Polym Sci A: Polym Chem 1993;31:2493.
[12] Lan T, Kaviratna PD, Pinnavaia TJ. Chem Mater 1994;6:573.
[13] Tyan HL, Liu YC, Wei KH. Polymer 1999;6:573.
[14] Tyan HL, Liu YC, Wei KH. Chem Mater 1999;11:1942.
[15] Wang Z, Pinnavaia TJ. Chem Mater 1998;10:3769.
[16] Zilg C, Thomann R, Mulhaupt R, Finter J. Adv Mater 1999;11:49.
[17] Chen TK, Tien YI, Wei KH. J Polym Sci A: Polym Chem 1999;37:2225.
[18] Chen TK, Tien YI, Wei KH. Polymer 2000;41:1345.
[19] Messersmith PB, Giannelis EP. J Polym Sci A: Polym Chem 1995;33:1047.
[20] Yangchuan KE, Chenfen L, Zongneng QI. J Appl Polym Sci 1999;71:1139.
[21] Seymour RW, Estes GM, Cooper SL. Macromolecules 1970;3:579.
[22] Miller JA, Lin SB, Hwang KS, Wu KS, Gibson PE, Cooper SL. Macromolecules 1985;18:32.
[23] Kajiyama T, Macknight WJ. Macromolecules 1969;3:254.
[24] Wang CB, Cooper SL. Macromolecules 1983;16:775.
[25] Paik Sung CS, Hu CB, Wu CS. Macromolecules 1980;13:111.
[26] Vaia RA, Teukolsky RK, Giannelis EP. Chem Mater 1994;6:1017.
[27] Hwang KK, Wu SG, Lin SB, Cooper SL. J Polym Sci: Polym Chem Edi 1984;22:1677.
[28] Martin DJ, Meijs GF, Renwick GM, Gunatillake PA, Mccarthy SJ. J Appl Polym Sci 1996;60:557.
[29] Zhang B, Tan H. Eur Polym J 1998;34:571.
[30] Pimentel GC, Mcclellan AL. The hydrogen bond. San Francisco, CA: Freeman, 1960 (p. 136).
[31] Meuse CW, Yang X, Yang D, Hsu SL. Macromolecules 1992;25:925.